JCTC Journal of Chemical Theory and Computation

Article

pubs.acs.org/JCTC

Evaluation of the Role of Water in the H_2 Bond Formation by Ni(II)-Based Electrocatalysts

Ming-Hsun Ho, Simone Raugei,* Roger Rousseau, Michel Dupuis,* and R. Morris Bullock

Center for Molecular Electrocatalysis, Pacific Northwest National Laboratory, P.O. Box 999, K1-83, Richland, Washington 99352, United States

Supporting Information

ABSTRACT: We investigate the role of water in the H−H bond formation by a family of nickel molecular catalysts that exhibit high rates for H_2 production in acetonitrile solvent. A key feature leading to the high reactivity is the Lewis acidity of the Ni(II) center and pendant amines in the diphosphine ligand that function as Lewis bases, facilitating H−H bond formation or cleavage. Significant increases in the rate of H_2 production have been reported in the presence of added water. Our calculations show that molecular water can displace an acetonitrile solvent molecule in the first solvation shell of the metal. One or two water molecules can also participate in shuttling a proton that can combine with a metal hydride to form the H−H bond. However the participation of the water molecules does not lower the barrier to H−H bond formation. Thus these calculations suggest that the rate increase due to water in these electrocatalysts is not associated with the elementary step of H−H bond formation or cleavage but rather with the proton delivery steps. We attribute the higher barrier in the H−H bond formation in the presence of water to a decrease in direct interaction between the protic and hydridic hydrogen atoms forced by the water molecules.

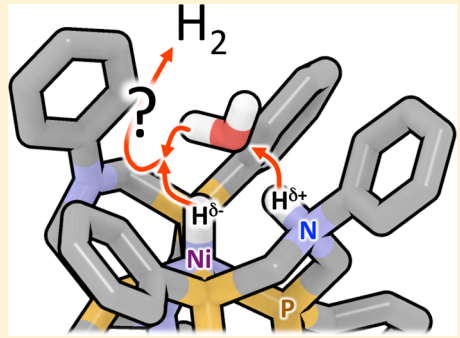

INTRODUCTION

Recent studies carried out on molecular Ni-based molecular electrocatalysts for H_2 oxidation or production[1−3] showed that molecular water[4] significantly accelerates the rate of catalysis in acetonitrile solvent. The catalytic cycles have been shown to involve a series of chemical and electrochemical steps. In this paper, we focus on the chemical steps, in particular the heterolytic cleavage or formation of the H−H bond (Scheme 1), and we aim to understand whether molecular water is responsible for the rate increase of this elementary step, and possibly in the overall catalytic rate.[5−8]

Scheme 1

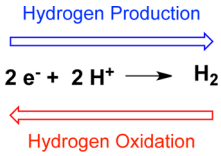

From a broader perspective, activation and formation of molecular hydrogen are processes of tremendous fundamental importance in chemistry[9,10] as well as in practical areas of applications, such as energy storage, delivery, and utilization.[11] Homogeneous catalysis offers promising venues for renewable energy-related H_2 chemistry.[1,2,12−16] Many studies of H_2 reactivity with organometallic compounds, and more recently by metal-free catalysts, have involved nonaqueous media,[17−19] though recent studies have reported water-soluble compounds.[20−24] However, H_2 chemistry in aqueous solution is of particular interest because of environmental and economic advantages. Accordingly, there is interest in understanding the role of molecular water on the reactivity occurring in nonaqueous solvents. As a protic, highly polar molecule that engages in hydrogen bonds, molecular water often interacts strongly with the reacting species (reactants, products, and transition states) and is known to promote reactivity.[25,26] As a solvent, water is also know to affect drastically reaction kinetics (faster or slower) by stabilizing or destabilizing the transition state with respect to reactants and products through differential interactions affecting charge separation.[27−30]

Several recent computational studies have been devoted to understanding the role of molecular water in participating in metal-based H_2 activation or formation.[21,31−34] A density functional theory (DFT) study carried out by Peruzzini and co-workers reported that water assists in the heterolytic H−H splitting catalyzed by water-soluble $[CpRu(PTA)_2Cl]$ (PTA = 1,3,5-triaza-7-phosphaadamantane).[31] These authors suggested that a proton wire involving a three water bridge is necessary to connect the proton acceptor and donor in the catalyst, i.e., the metal center and one of the amino functions in the PTA ligand, in order to cleave H_2. Similarly, Yoshizawa and co-workers suggested that water directly bridges a Ru-bound hydride to a C−H hydrogen and lowers the activation barrier to H_2 formation with a Ru(II) tridentate PNN pincher complex in

Received: May 14, 2013

   dx.doi.org/10.1021/ct400396s | J. Chem. Theory Comput. XXXX, XXX, XXX−XXX

aqueous solution.[32] Beyond these studies, there is insufficient experimental and theoretical evidence regarding a general role of water in facilitating H_2 splitting or evolution. The present paper adds to the understanding of how molecular water can influence these processes. We compare our findings relevant to the series of Ni-based electrocatalysts developed in our Center to those for the Ru-based systems mentioned above. In particular, both types of metal catalysts have similar chemical proton acceptor and donor functionalities. It will be shown that molecular water does not accelerate the chemical steps in our Ni-based catalysts with pendant amines, in contrast to what is reported for the Ru-based catalysts; we rationalize these findings on the basis of electronic structure considerations.

Recent experimental studies have revealed that water accelerates the electrocatalytic H_2 oxidation[35] and H_2 production by $[Ni(P^R_2N^{R'}_2)_2]^{2+}$ complexes (P_2N_2 = 1,5-diaza-3,7-diphosphacyclooctane, Figure 1) and H_2 production[7,36,37]

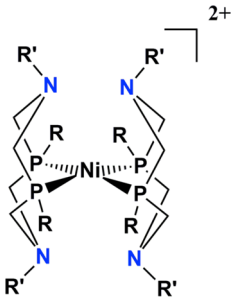

Figure 1. A schematic representation of $[Ni(P^R_2N^{R'}_2)_2]^{2+}$. The six-membered rings are shown in their boat conformations. R and R′ are phenyl groups in this study.

by $[Ni(7P^R_2N^{R'})_2]^{2+}$ ($7P_2N$ = l-aza-3,6-diphosphacycloheptane) complexes.[8] These nickel(II)-bis(diphosphine) catalysts exhibit high rates and feature one or two pendant amines in the diphosphine ligand, the second coordination sphere of the metal, which is related to amines found in many metalloenzymes, such as [FeFe] and [NiFe] hydrogenases.[38−40] These electrocatalysts are stable and soluble in water−organic solvent mixtures.[6,41] Finally, it has been observed experimentally that water in concentrations up to the molar regime in organic solvents increases the rates of H_2 production, in some cases by more than a factor of 50.[7,36] For example, Kilgore et al.[7] reported that for the H_2 production catalyst $[Ni(P^R_2N^{R'}_2)_2]^{2+}$ (Figure 1) with R = Ph and R′ = $C_6H_4CH_2P(O)(OEt)_2$, using protonated dimethylformamide (DMF) as the proton source, the turnover frequency (TOF) is 500 s^{-1} in dry acetonitrile and 1850 s^{-1} in the presence of 0.2 M water. Using similar experimental conditions, Helm et al.[8] observed for the $[Ni(7P^R_2N^{R'})_2]^{2+}$ catalyst an increase of TOF from 33 000 s^{-1} under dry conditions to 106 000 s^{-1} in the presence of 1.2 M water.

Previous computational studies[42,43] of $[Ni(P^R_2N^{R'}_2)_2]^{2+}$ showed that H_2 oxidation proceeds with the formation of a transient, loosely bound H_2 adduct (**A**), which promptly undergoes heterolytic H_2 splitting leading to the formation of a N-protonated nickel hydride species (proton/hydride species, **PH**). The latter easily evolves toward a doubly protonated Ni(0) species (**PP**). Removal of two protons and two electrons (possibly proceeding through proton-coupled electron transfers[44−46]) completes the catalytic cycle (Scheme 2). H_2 evolution follows the same cycle (counterclockwise in Scheme 2), with the initial steps being the two reduction/protonation steps. In this case, the reaction proceeds downhill toward the release of molecular hydrogen. The pendant amines facilitate intramolecular[47] and intermolecular[48] proton transfers. Recent experimental and theoretical studies indicated that the monoprotonated $[Ni(P^R_2N^{R'}_2)(P^R_2N^{R'}_2H)]^+$ species formed after the first protonation is not stable and undergoes fast proton transfer from nitrogen to the metal, generating $[HNi(P^R_2N^R_2)_2]^+$.[48,49] Considering **PH**s are more stable than **PP**s in the case of H_2 production catalysts,[49] it is likely that upon a second protonation, **PH**s are directly formed without the involvement of **PP**s (Scheme 2).

Our laboratory has been working on these promising pendant amine-based electrocatalysts for several years. Despite the remarkable progress in understanding the catalytic

Scheme 2. The Catalytic Cycle for H_2 Oxidation (Clockwise) and H_2 Production (Counterclockwise) by $[Ni(P^R_2N^{R'}_2)_2]^{2+}$ Catalysts[a]

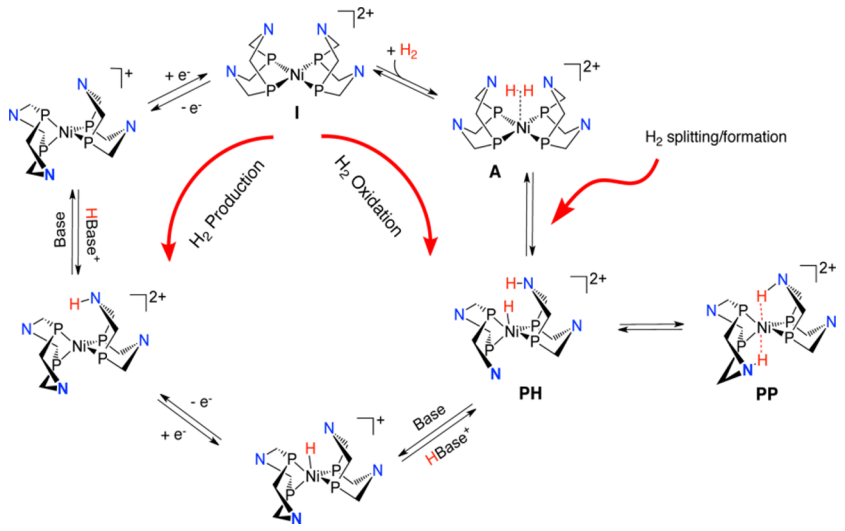

[a]For clarity, R and R′ groups are not shown.

dx.doi.org/10.1021/ct400396s | J. Chem. Theory Comput. XXXX, XXX, XXX−XXX

mechanism, it is still unclear what the rate-determining step(s) is (are). We know that proton delivery to the pendant amines (H_2 production) or from the pendant amines (H_2 oxidation) is important.[48] In the case of H_2 production, the presence of multiple protonation sites can populate different isomers, not all of them catalytically competent.[6] In the case of H_2 oxidation, H_2 splitting or the subsequent deprotonation can be rate-determining.[48,49] In principle, water can either help proton delivery and removal or facilitate H−H bond formation and breaking as reported in the literature for other organometallic complexes. This paper considers whether molecular water accelerates the rate of H_2 evolution by reducing the barrier to H_2 formation from the proton-hydride intermediate **PH**. To this end, we must characterize the solvent structure in the first solvation shell of the catalyst, in particular inside the catalytic pocket. We then need to quantify the ability of water molecules to displace the solvent inside the catalytic pocket. Finally, we need to determine the mechanism by which molecular water(s) get involved in the transition state for the H−H bond formation/cleavage step, and how this affects the activation barrier. Throughout this study, the challenge is how to treat accurately this specific interaction between the catalyst and the hydrogen bonded solvent or the water molecules. Our approach has been to carry out mixed Hamiltonian density functional theory (DFT)/molecular mechanics (QM/MM) simulations[50] and to combine them with stationary point searches on the DFT potential energy surface. We studied the extensively characterized H_2 production catalyst $[Ni(P^{Ph}_2N^{Ph}_2)_2]^{2+}$ (with R = R′ = Ph). With 2,6-dichloro-anilinium as acid, this catalyst shows a TOF of 31 s^{-1} in dry acetonitrile and 160 s^{-1} in an acetonitrile solution containing 1 M water,[7] which corresponds to a decrease of the overall (apparent) activation barrier for the formation of H_2 of about 1.0 kcal/mol in the presence of water. Experimentally the observed kinetics cannot distinguish between first- or second-order in water.[7] Accordingly, we investigated reaction mechanisms involving one or two water molecules. Our study shows that molecular water can indeed bind to **PH** and participate in the transition state for H−H bond formation/cleavage in two different ways: (*i*) acting as a shuttle for a proton from the protonated amine to the Ni-hydride or (*ii*) acting as a H-bonding acceptor during the direct bond formation between the proton on the amine and the hydridic hydrogen on the Ni center. *The energy barrier in the elementary step of H−H bond formation is appreciably higher in the former case, when one or more water molecules act as a proton shuttle*. This finding, which is in contrast to studies referenced earlier, suggests that the H−H bond formation is not rate determining and that water participating in the chemical steps of the catalytic cycle is not the reason for the overall catalytic rate increase. The observed rate increases from molecular water in this class of catalysts must come from the effect of molecular water on other steps, i.e., the proton delivery steps from (to) a base to (from) the catalysts, and that those steps must be rate-determining. This hypothesis about the role of molecular water on proton delivery/removal will be the subject of future research.

METHODS

Definition of Models. In this work, we considered several models containing up to two water molecules, with or without one additional explicit acetonitrile (CH_3CN) solvent molecule included. The reason for including one explicit acetonitrile molecule in the models lies in the fact that, in pure acetonitrile solvent, one acetonitrile molecule is directly interacting with the functional groups in the catalytic pocket.[48] The water molecules must displace this first-shell acetonitrile solvent molecule to establish direct interactions with the metal center and/or the pendant amine. Molecular acetonitrile and molecular water interact with these Lewis acid and base sites by hydrogen bonds. Accordingly, the stable configurations and intermediates are the results of a delicate balance between the strengths of these hydrogen bond interactions.

Among the possible conformers of the **PH** (proton-hydride) species, we selected the lowest energy isomer where the N−H bond of the protonated pendant amine is directed toward the hydridic hydrogen (H^-).[49] The protic hydrogen on the pendant amine will be denoted H^+. In what follows, we adopt the notation **PH·S** to represent the proton/hydride species with either a solvent molecule (**S** = CH_3CN) or a water molecule (**S** = H_2O) interacting with the metal catalyst. Similarly, we denote **TS·S** as the corresponding transition state for H_2 formation (or splitting in H_2 oxidation reaction) and **A·S** the H_2 adduct. Specifically, we focused on the H−H bond formation starting from the **PH** intermediate under the following conditions: (*i*) no explicit acetonitrile or water molecules included (**PH**, Figure 2A)—akin to the structure *in vacuo*—while informative, this model is not sufficient to address the question to quantify the ability of water molecules to displace acetonittrile and interact with the active site; (*ii*) one acetonitrile molecule interacting with H^+ and H^- in the catalytic pocket (**S** = CH_3CN, Figure 2B); (*iii*) same as *ii* but with acetonitrile replaced by one water molecule (**S** = H_2O, Figure 3A); (*iv*) same as in *ii* with one water molecule and one acetonitrile molecule together (**S** = $H_2O{\cdot}CH_3CN$, Figure 3B); (*v*) same as in *ii* with two water molecules in the catalytic pocket (**S** = $H_2O{\cdot}H_2O$, Figure 4A), with the second water molecule not directly interacting with the catalysts; (*vi*) same as in *v* but with the second water molecule interacting with the

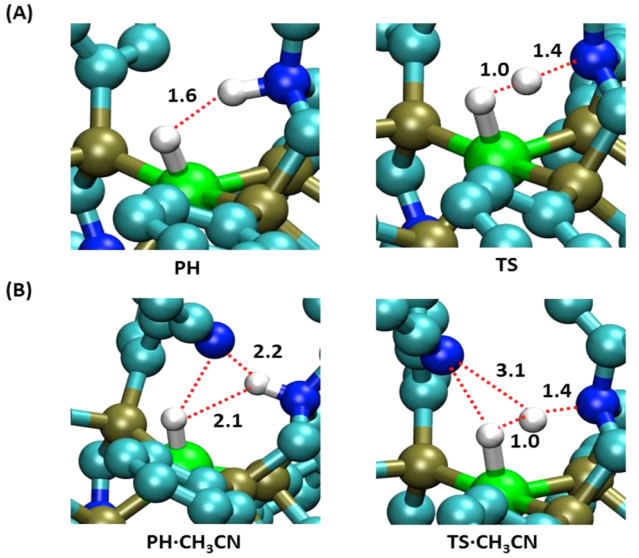

Figure 2. Proton hydride (**PH**) and transition state (**TS**) structures in the H−H bond formation. In the top panels (A), acetonitrile as a solvent is described by a polarizable continuum model. In the bottom panels (B), one explicit acetonitrile molecule is shown hydrogen bonded to the protonated pendant amine. Key interactions involving hydridic and protic hydrogen atoms are depicted with a dashed line. Selected distances are in Å.

dx.doi.org/10.1021/ct400396s | J. Chem. Theory Comput. XXXX, XXX, XXX−XXX

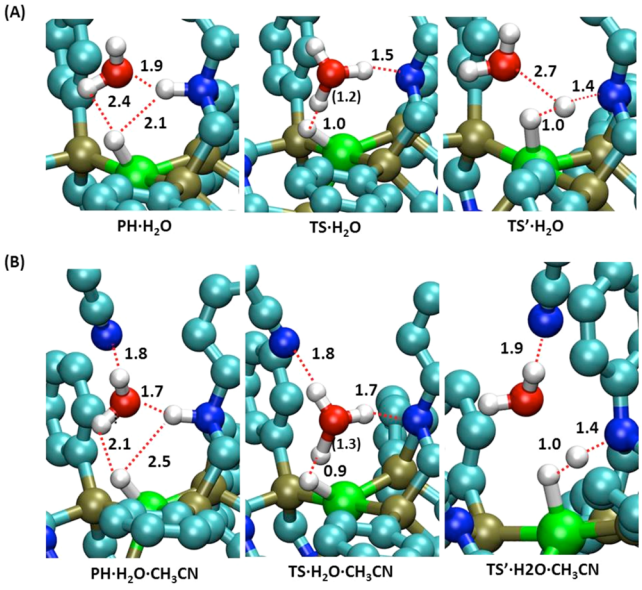

Figure 3. Proton hydride (**PH**) and transition state (**TS** and **TS′**) structures in the H−H bond formation involving one water molecule: (A) The top panels show the water molecule hydrogen bonded to the protic and hydridic hydrogen atoms in **PH·H_2O**. **TS·H_2O** depicts the shuttling of the proton through the water molecule to form the H−H bond, while in **TS′·H_2O** there is a direct transfer between the hydridic and protic hydrogen atoms. (B) As in A with one solvent acetonitrile molecule added. Acetonitrile is hydrogen bonded to the dangling O−H bond of the water molecule in all three structures. The hydrogen bonds between water, acetonitrile, and the amine proton are shown as dashed lines. Selected distances are reported in Å. The O−H bond lengths in the hydronium moiety in the transition state **TS·H_2O** are also shown in parentheses.

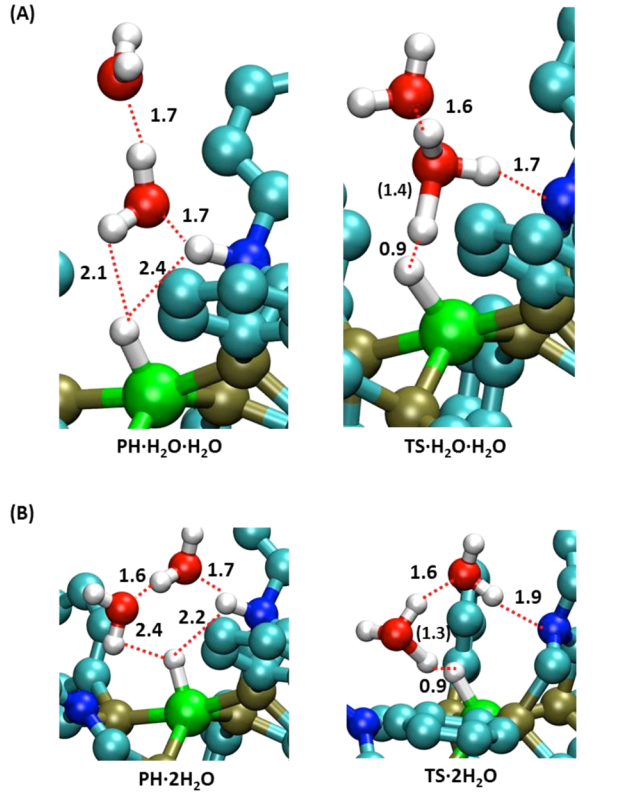

Figure 4. Proton hydride (**PH**) and transition state (**TS**) structures in the H−H bond formation assisted by two water molecules: (A) The top panels show one water molecule hydrogen bonded to the protic and hydridic hydrogen atoms, while the second water molecule is hydrogen bonded to the active water molecule (**S** = **$H_2O·H_2O$**). (B) The bottom panels show two water molecules interacting with the protic and hydridic hydrogen atoms (**S** = **$2H_2O$**). The two water molecules are involved in the shuttling of two protons, one from the amine to the proximal water, the other one between the two water molecules. The hydrogen bonds involving the water molecules and the protic and hydridic hydrogen atoms are shown as dashed lines. Selected distances are reported in Å. The O−H bond lengths of the hydronium species in the transition state are shown.

hydridic hydrogen H^- (**S** = $(H_2O)_2$, Figure 4B), and the two water molecules forming a proton wire between H^- and H^+.

Electronic Structure Methods. DFT calculations were carried out to characterize the stationary points (reaction intermediates and transition states) involved in the H−H bond formation/cleavage from/to the proton-hydride **PH** species in $[Ni(P^{Ph}{}_2N^{Ph}{}_2)_2]^{2+}$ (Scheme 2). The six-membered ring involving the Ni−P−C−N−C−P atoms (Figure 1) can adopt either a chair or a boat conformation. Considering the four six-membered rings in the complex and neglecting conformations such as skew boats, a total of seven chair/boat conformers can be defined. To remain consistent with previous investigations,[42,43,49] we chose the all-boat conformer. This choice is supported by the earlier studies of the H_2 oxidation catalyst $[Ni(P^{Cy}{}_2N^{Me}{}_2)_2]^{2+}$ showing that the activation barrier for the elementary H−H bond formation/cleavage step is not significantly affected by the conformation of the rings associated with the other pendant amines. All structures were optimized using DFT with the B3P86 hybrid[51,52] functional along with the Stuttgart−Dresden relativistic effective core potential and the associated basis set (SDD) for Ni.[53] The polarized double-ζ 6-31G* basis sets were used for the nonmetal atoms. The 31G* basis set with one *p*-polarization function was used for the protic and hydridic H atoms.[54] The solvation energy in acetonitrile solvent for each optimized structure was calculated using the C-PCM model,[55,56] denoted as PCM below (dielectric constant =35.7), in connection with the Bondi radii[57] with no scaling factor applied. This level of theory has been tested extensively in previous studies and proved to work well for this class of compounds.[43] Specifically, for the $[Ni(P^{Me}{}_2N^{Me}{}_2)_2]^{2+}$ catalyst, the difference in the barrier for H_2 formation from the **PH** intermediate between DFT/B3P86 and CCSD(T) calculations is only ∼1.2 kcal/mol. In addition, for a given DFT exchange and correlation functional, we expect a systematic error cancellation for species with varying numbers of water and acetonitrile molecules. Therefore, differences in energies of possible stationary points along the catalytic pathway with and without water are expected to be meaningful. Harmonic vibrational frequencies were calculated for all optimized structures using the same level of theory to estimate the associated free energy under room conditions. The reactant and product states were confirmed by all positive vibrational frequencies and transition states by one imaginary frequency only and the associated normal mode leading to the H−H bond formation/cleavage. Intrinsic Reaction Coordinate (IRC) calculations[58] were carried out in all cases to confirm the reaction pathway.

Nuclear quantum effects can play an important role in the proton transfer process. In the present study, we only considered zero point energy nuclear effects, as previous

dx.doi.org/10.1021/ct400396s | J. Chem. Theory Comput. XXXX, XXX, XXX−XXX

studies showed that the hydrogen tunneling plays a minor role at room temperature for this reaction.[48]

All of the calculations described in this section were performed with the program Gaussian 09.[59] The relative energies and free energies for all the species are reported in Table 1. The free energy profiles for selected systems are shown in Figure 5.

Table 1. Energies [$\Delta E_{(solv)}$] and Free Energies [$\Delta G_{(solv)}$] of the Various Model Systems in Acetonitrile Solvent for the Formation of the Di-Hydrogen (PH to A step) Relative to the Energies of PH[a]

		ΔE(solv) kcal/mol	ΔG(solv) kcal/mol	TS freq. (cm^{-1})
PH → A	TS direct	9.7	6.4	i 854
	A	4.9	1.5	
PH·CH_3CN → A·CH_3CN	TS direct	11.2	5.7	i 843
	A	4.3	−2.9	
PH·H_2O → A·H_2O	TS shuttle	14.2	10.7	i 898
	TS′ direct	11.5	8.2	i 909
	A	6.5	3.0	
PH·H_2O·CH_3CN → A·H_2O·CH_3CN	TS shuttle	12.3	10.1	i 607
	TS′ direct	11.7	7.0	i 870
	A	7.3	4.4	
PH·H_2O·H_2O → A·H_2O·H_2O	TS shuttle	9.1	10.4	i 552
	A	6.3	6.7	
PH·$2H_2O$ → A·$2H_2O$	TS shuttle	15.9	13.0	i 463
	A	8.7	3.8	

[a]The imaginary frequencies of the transition state mode for the transition state structures depicted in Figures 2−4 are also reported.

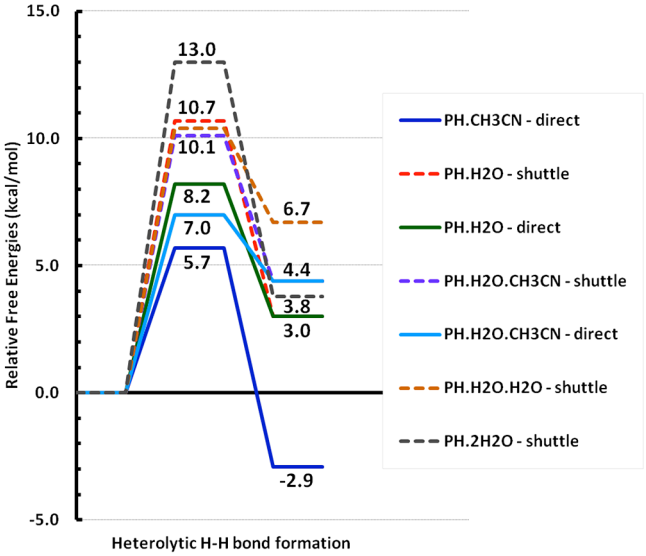

Figure 5. Free energy profiles relative to **PH** for H−H bond formation in the **PH** to **A** elementary step for the different models. The solid lines are for "direct" reactions of the amine proton and hydridic hydrogen to form the H−H bond in the presence of molecular acetonitrile and water(s). The dotted lines are for reactions in which water molecules act as proton shuttles.

Calculation of the Binding Energy of Molecular Acetonitrile and Water to the Active Site. Prior to characterizing the reactive steps of interest, it is important to understand the equilibrium interactions between a first solvent shell acetonitrile molecule and the active site and between water molecules and the active site. While PCM models seem appropriate to obtain a consistent treatment of bulk solvation effects on the *intramolecular* process of H−H bond formation/cleavage for the models *i*−*vi* above, their use to characterize *intermolecular* processes, such as dissociation and association, is more problematic.[60−63] The challenge is most strongly experienced when the solute can engage in specific interactions (i.e., hydrogen bonds) with the solvent. In the present case, the protic and hydridic hydrogens of the proton-hydride species **PH** engage in hydrogen bonds with an acetonitrile solvent molecule, and with the water molecule(s).

In order to obtain an accurate estimate of the differences in binding to **PH** for these two cases, **PH·CH_3CN** ⇆ **PH** + CH_3CN and **PH·H_2O** ⇆ **PH** + H_2O, we resorted to the use of a hybrid quantum mechanics/molecular mechanics (QM/MM) level of theory combined with molecular dynamics (MD) simulations. Binding free energies can be obtained from such MD simulations using enhanced sampling techniques.[77] In the present studies, the MD simulations were carried out as follows. The Ni catalyst was embedded in a mixture of 60 water molecules and 956 acetonitrile molecules in a cubic box size of 44.7 Å × 44.7 Å × 44.7 Å, corresponding to the following concentrations: 0.02 M for the nickel complex, 1.13 M for water, and 17.76 M for acetonitrile (the concentration of pure acetonitrile is 19.15 M). These are similar to typical concentrations employed in the experiments. The system was equilibrated for 2 ns at constant pressure[64] and constant temperature[65] using a force field description[66] (including for the Ni catalyst) and keeping the Ni catalyst frozen in its gas-phase optimized structure. The procedure adopted for these simulations was described previously.[48] Two configurations, one with an acetonitrile molecule bound to H^+ and one with a water molecule bound to H^+, were extracted from these force field-based MD trajectories and used as initial configurations for the subsequent QM/MM calculations. In the QM/MM calculations, the Ni complex and either the acetonitrile molecule or the water molecule(s) bound to it were treated at the QM (DFT) level of theory. The electrostatic interactions between the QM and MM subsystems were described by a real space, multigrid, linear scaling coupling scheme.[67] Each system was then relaxed at the QM/MM level of theory and equilibrated at a constant volume and constant temperature for 2 ps using an integration time step of 0.25 fs. The QM/MM simulations were carried out within the DFT framework using the hybrid Gaussian and plane waves (GPW) method implemented in the CP2K code.[68] A triple-ζ basis set augmented with two sets of *d*-type and *p*-type polarization functions was employed for the valence electrons of all the atoms (TZV2P basis set).[69] The interaction between valence and core electrons was described using norm-conserving pseudopotentials.[70] The electrostatic energy was calculated using an auxiliary plane wave basis set with a cutoff energy of 280 Ry in a 27 × 27 × 27 $Å^3$ periodic cubic box. The Perdew−Burke−Ernzerhof (PBE) exchange and correlation functional[71] was employed along with Grimme's correction for dispersion interactions (PBE+D).[72] Previous calculations showed that the PBE+D level of theory yields good descriptions of the energetics associated with the $[Ni(P^R{}_2N^{R'}{}_2)_2]^{2+}$ catalysts and

dx.doi.org/10.1021/ct400396s | J. Chem. Theory Comput. XXXX, XXX, XXX−XXX

gives results comparable to those obtained with the hybrid B3P86 functional.[49] The MM solvent acetonitrile was described using the empirical potential by Nikitin and Lyubartsev,[73] while the TIP3P potential model was employed for water.[74]

The binding free energy of molecular acetonitrile or water to **PH** was estimated by computing the potential of mean force for the unbinding process via constrained molecular dynamics simulations.[75] The distance between the N atom of the acetonitrile molecule or the O atom of the water molecule to the metal center was chosen as the reaction coordinate. Simulations for 15 different distances from about 3 Å to 6 Å were carried out. For each window, the simulation time varied from 5 to 15 ps. Simulations were started from the hydrogen bonded complexes, i.e., **PH·CH$_3$CN** or **PH·H$_2$O**.

RESULTS

We first consider the issue of whether a water molecule can easily displace an acetonitrile molecule in the first solvation shell of the proton-hydride **PH** form of the catalytic species. The results (Figure 6) indicate that water and acetonitrile bind

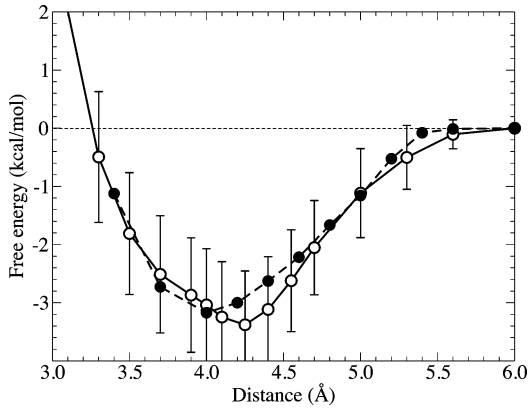

Figure 6. Free energy profiles for the binding of molecular water (open circles) and acetonitrile (filled circles) to **PH** as a function of the distance between the metal center and the oxygen atom of water or the nitrogen atom of acetonitrile. The statistical uncertainty in the free energy for the binding of water is depicted as error bars. The statistical uncertainty for molecular acetonitrile is not shown for clarity, but it is of the same magnitude.

essentially as strongly to a bare **PH** species and thus that water can indeed displace acetonitrile to gain a reactive position. It follows that we can use the **PH·CH$_3$CN** and **PH·H$_2$O** species as reference points from which we can make conjectures about H−H bond formation starting from the proton-hydride **PH** species and ending at the adduct species **A**. To that end, we systematically characterize the elementary reaction pathways **PH·S** to **A·S** via **TS·S** where **S** is acetonitrile or water (or a combination of both) for the various models. The structures are depicted in Figures 2−4. The free energy results are given in Table 1 and are displayed in Figure 6 relative to **PH·S**, with **PH·S** in all the cases taken as the zero of (free) energy. The ensuing relative energies of the **A·S** species vs **PH·S** are qualitatively analyzed in terms of electrostatic (charge-dipole) and hydrogen bond interactions between **A** and **S**. From the stability of **A·S** relative to **PH·S**, we analyze in qualitative terms the magnitude of the activation barrier **A·S** using Bells−Evans−Polanyi considerations.[76]

Free Energies of Binding of Molecular Acetonitrile and Water to the Active Site. The interaction between acetonitrile or water with the molecular catalyst is attractive throughout from a distance of ∼6.0 Å down to ∼4.1 Å between the substrate and **PH**, the latter distance corresponding to a local minimum on the free energy surface of the systems (Figure 6). Both substrates display similar binding free energies to **PH** (ΔG_{H2O} = −3.4 kcal/mol and ΔG_{CH3CN} = −3.2 kcal/mol). The difference between the two binding energies is smaller than the statistical uncertainty of the MD averages, which we estimated to be ∼1.0 kcal/mol. After standard state correction, RT log Q^{sim}/Q^0, where Q^{sim} is the concentration ratio for the association reaction in the simulation conditions and Q^0 is the concentration ratio in the standard state conditions, we obtain $\Delta G_{H2O}{}^0$ = −3.3 kcal/mol and $\Delta G_{CH3CN}{}^0$ = −3.3 kcal/mol (Q^{sim} and Q^0 are 17.73 and 19.15 for the binding of molecular acetonitrile; Q^{sim} and Q^0 are 1.13 and 1.0 for the binding of molecular water).

In summary, our calculations suggest that the exchange reaction between molecular acetonitrile and molecular water in the first solvation sphere of the **PH** intermediate is thermoneutral. In spite of the small binding free energy, the residence time at room temperature of molecular acetonitrile, and more importantly of molecular water in the catalytic pocket, can be estimated using simple transition state theory arguments to be of a few tens of picoseconds, much shorter than the reaction time for H−H bond formation. This is an important finding with regard to the validity of the models in yielding a realistic description of the H−H bond formation/cleavage. The ensuing findings about the changes in magnitude of activation barriers can thus be used to assess the role of molecular water in accelerating or not the H−H bond formation/cleavage step.

H−H Bond Formation in the Presence of Acetonitrile. We first comment on the model with no explicit acetonitrile molecules included, and the acetonitrile solvent is represented by the PCM model. This illustrates how a dielectric continuum model of solvation does not represent well specific solute−solvent interactions.

The H−H bond formation reaction starting from **PH** to form the Ni(II) catalyst plus an infinitely separated H_2 molecule is calculated to be exothermic by 10.6 kcal/mol (free energy), in satisfactory agreement with the experimental value of 9.0 kcal/mol at 298 K and 1 atm.[77] Although identified as a local minimum on the energy surface, the dihydrogen adduct **A** is given by the PCM model to lie 1.5 kcal/mol higher in free energy than **PH**, in contrast to −2.9 kcal/mol for **A·CH$_3$CN** relative to **PH·CH$_3$CN** when the acetonitrile molecule in the first solvent shell is described explicitly.

The activation barrier for the H−H bond formation with the **PH**-only model with PCM is calculated to be 6.4 kcal/mol, compared to 5.7 kcal/mol when one acetonitrile solvent molecule (hydrogen bonded to H^+) is explicitly included in the calculation in addition to the continuum solvent (Table 1). The structures of **PH** and **PH·CH$_3$CN** and the corresponding transition states are shown in Figure 2. The optimized structure of the **PH·CH$_3$CN** complex (embedded in the PCM continuum) is very similar to the structure obtained from the solvent-explicit MD simulations. One major structural change between **PH** and **PH·CH$_3$CN** consists of a longer H^+/H^- distances in the latter (1.6 Å vs 2.1 Å). The elongation of H^+/H^- distances is due to the shielding by the explicit acetonitrile molecule of the direct (electrostatic and hydrogen bond) interaction between the proton on the amine and the hydridic hydrogen on Ni. In **PH·CH$_3$CN**, the hydrogen bond distance

dx.doi.org/10.1021/ct400396s | J. Chem. Theory Comput. XXXX, XXX, XXX−XXX

between H^+ and the N atom of acetonitrile is 2.2 Å. In addition, the orientation of the N−H^+ bond is altered, toward the CH_3CN molecule in **PH·CH$_3$CN** and less toward the hydridic hydrogen as in **PH**. Regardless of these nuances, we note that the H^+/H^- distance is significantly shorter in these catalysts than in the Ru-based H_2 production catalysts mentioned in the Introduction.[31] This observation is an essential factor contributing to the differences in the role and effect of molecular water in the H−H formation step for the present Ni-based platform of catalysts in contrast to the Ru catalysts, and this will be further discussed below.

H−H Bond Formation Assisted by One Water Molecule. Even though the binding energies of acetonitrile and molecular water to **PH** are very similar, the structures of **PH·CH$_3$CN** and **PH·H$_2$O** show marked differences: molecular acetonitrile exhibits interaction with the amine proton (N···H^+ ∼ 2.2 Å) only, whereas molecular water interacts with both the amine proton (O···H^+ ∼ 1.9 Å) and the hydride on the Ni center (H_{H2O}···H^- ∼ 2.4 Å). Due to its small size, the water molecule can easily reorient and form a stronger hydrogen bond with the amine proton. Specifically, the O·H−N^+ hydrogen bond in **PH·H$_2$O** is shorter and more linear (140.0°), compared to that in PH·CH_3CN (128.7°). This is likely what makes the binding energy of molecular water similar to that of acetonitrile (see section above) in spite of the dipole moment of acetonitrile is about twice the dipole moment of water (3.9 vs 1.8 D). Overall, the structures of **PH** in **PH·H$_2$O** and **PH·CH$_3$CN** are similar.

Two reaction pathways for the formation of the H−H bond in the presence of one water molecule were found. In the first one, labeled **TS·H$_2$O** (Figure 4A), water acts as a proton shuttle, accepting the proton from the protonated amine and donating a proton from water to the nickel hydride to form the H−H bond. The transition state for this pathway is indeed characterized by a hydronium-like moiety with the H_{water}/H^- distance appreciably shorter than the corresponding H_{water}/O_{water} distance (1.0 Å and 1.2 Å, respectively) suggesting a late transition state. The activation free energy for the elementary step of H−H bond formation is 10.4 kcal/mol, appreciably larger than the value of 5.7 kcal/mol calculated for the **PH·CH$_3$CN** system, for which we describe the process as "direct" (Table 1 and Figure 6). The further addition in **TS·H$_2$O** of an explicit CH_3CN solvent molecule, hydrogen bonded to the dangling water OH bond (**TS·H$_2$O·CH$_3$CN**, Figure 3B), causes a slight decrease of the activation free energy to 10.1 kcal/mol (Table 1 and Figure 6). Such a barrier is still larger by 4.4 kcal/mol than the "reference" barrier in **PH·CH$_3$CN** when no water molecules are present. Therefore, the pathways where molecular water serves as a proton shuttle are appreciably less favorable than the "direct" formation of H_2 in acetonitrile only.

The second pathway when a water molecule is present closely resembles the "direct" pathway for H−H formation in **PH·CH$_3$CN**, with the water molecule remaining hydrogen bonded to the amine proton H^+ from **PH** all the way up to **TS**, and not participating directly in the formation of the H−H bond (pathway 2, Figure 3A). An activation barrier of 8.2 kcal/mol was calculated for this pathway, labeled **TS′·H$_2$O**. This value is smaller than that for the first pathway (10.1 kcal/mol) but higher than the barrier in acetonitrile only in the absence of water (5.7 kcal/mol, Table 1). The similarity between the species **TS·CH$_3$CN** and **TS′·H$_2$O** is very strong from a structural point of view, yet the barrier in the latter case is significantly higher. This can be rationalized by considering the stability of **A·H$_2$O** relative to **PH·H$_2$O** compared to the stability of **A·CH$_3$CN** relative to **PH·CH$_3$CN** (Table 1 and Figure 6). **A·H$_2$O** is less stable relative to **PH·H$_2$O** than **A·CH$_3$CN** relative to **PH·CH$_3$CN**. The **A·H$_2$O** is a local minimum on the potential energy surface where the water molecule is stabilized inside the catalytic pocket by hydrogen bonding with the π-acceptor phenyl substituents (Figure SI1 and SI2). The data reported in Figure 6 refer to this local minimum.

The addition of an explicit molecule of acetonitrile hydrogen bonded to the dangling OH of water in the transition state (denoted **TS′·H$_2$O·CH$_3$CN** in Figure 3B) decreases the free energy barrier down to 7.0 kcal/mol (Table 1 and Figure 6), a value still higher than the barrier in the absence of water (5.7 kcal/mol in **PH·CH$_3$CN**).

H_2 Formation Assisted by Two Water Molecules. Two low energy structures of **PH** with two water molecules were found. The first structure, labeled **PH·H$_2$O·H$_2$O**, features one water molecule directly bound to **PH** with the second molecule hydrogen bonded to the dangling OH of the first water (Figure 4A). Upon inclusion of the second water molecule, the inner water molecule gets closer to the metal center with a lengthening of the H^+/H^- distance of 0.3 Å as a result of the increased shielding of the direct H^+/H^-. In the second structure, labeled **PH·(H$_2$O)$_2$**, the two water molecules form a wire connecting H^+ and H^- (Figure 4B), a situation similar to the one proposed for [CpRu(PTA)$_2$Cl·H_2].[31] The elementary step of H−H bond formation from **PH·H$_2$O·H$_2$O** is characterized by an activation barrier of 10.4 kcal/mol (with one water molecule acting as a shuttle) that is appreciably smaller than the barrier of 13.0 kcal/mol for the two water shuttle **PH·(H$_2$O)$_2$** (Table 1 and Figure 6). In conclusion, it is notable that the elementary step of H−H bond formation when two water molecules are involved exhibits a higher activation barrier than the pathway in the absence of water.

DISCUSSION AND CONCLUSIONS

Increases in rate of H_2 production up to 50 fold were observed experimentally in studies of $[Ni(P^{Ph}{}_2N^{C6H4X}{}_2)_2]^{2+}$ catalysts in the presence of 0.02 to 2.4 M of water.[7,36,37] These observations prompted our interest in understanding the role of molecular water. To this end, we carried out DFT studies of the H−H bond formation starting from a proton-hydride **PH** intermediate ($[HNi(P^{Ph}{}_2N^{Ph}{}_2)_2H]^{2+}$, Scheme 2). This study focused on the interactions of the water molecules with the **PH** species, the structures of the catalyst−water complexes, the pathways involving H−H bond formation, the associated transition states, and the relative stability of the products. Several models of **PH**/water complexes differing in the water content (zero, one or two molecules) were considered. We also investigated complexes that included an explicit acetonitrile molecule and complexes with both water and acetonitrile molecules.

We found that both molecular acetonitrile and water can form strong hydrogen bonds with the proton-hydride species **PH**. The binding free energies of molecular acetonitrile and molecular water are very similar (about 3 kcal/mol), and the lifetimes of the corresponding hydrogen-bonded species, i.e. **PH·CH$_3$CN** and **PH·H$_2$O**, are similar, indicating that water can compete with acetonitrile in binding to **PH** and also can displace acetonitrile from the proximity of the active site.

dx.doi.org/10.1021/ct400396s | J. Chem. Theory Comput. XXXX, XXX, XXX−XXX

We also have found that, in all the complexes where water is present, molecular water can bridge the protic hydrogen H^+ and hydridic hydrogen H^- and act as a proton shuttle in a Grotthuss-like mechanism[78] in the formation of the H−H bond. However, our calculations indicate that the barrier for these water-assisted H−H bond formation steps is higher than in the absence of water. Interestingly, in all the cases when molecular water is present, we identified also a second pathway referred to as "direct" where water does not act as a proton shuttle, but rather it remains a "spectator" in a direct H−H bond formation between the protic and hydridic hydrogen atoms. The activation barriers in the "shuttle" pathway are all higher than those in "direct" pathway in all of the systems we considered. The "direct" pathways have lower activation barriers than the "shuttle" pathways, but none have as low an activation barrier as the catalyst−acetonitrile complex. We assign this to the less stable adduct species **A** relative to the **PH** species in all cases when water is present and the concomitant increase in activation barrier consistent with the Bell−Evans−Polanyi rule. Since the lifetimes of **PH·CH$_3$CN** and **PH·H$_2$O** are comparable, and far shorter than the catalytic turnover times (picoseconds vs milliseconds), we conclude that the most likely mechanism for H−H bond formation (H_2 evolution) does not involve molecular water.

The effect of molecular water reported here contrasts with those discussed in recent reports, where molecular water was found to facilitate the H−H bond formation and cleavage by ruthenium-based catalysts.[31−33] As discussed in refs 19 and 20, if water is going to participate as a proton shuttle in a reactive step, it is anticipated in general that it will lower the activation barrier. The present work provides a counter-example in that the participation of water as a proton shuttle would give rise to an increased activation barrier. We attribute this result to the strong hydrogen bond interaction in the reactant state **PH** between the protic and hydridic hydrogens that is very conducive to "direct" H−H bond formation. Any insertion of molecular water as a shuttle breaks this favorable protic−hydridic interaction prior to providing a shuttling channel. The energy cost associated with the decrease in the interaction between the hydridic, H^-, and protic, H^+, hydrogen is not overcome by the shuttling opportunity as can be discerned from the values of ΔE(solv) and ΔG(solv) reported in Table 1, although the magnitude of the enthalpic penalty depends appreciably on the number of water and acetonitrile molecules explicitly included in the calculation. A direct protic−hydridic coupling is also possible in the presence of water, but even in this case this results in an increased activation barrier.

In the Ru-tridentate PNN pincer system discussed by Yoshizawa and co-workers,[32] the H^-/H^+ distance in the ground state (3.1 Å) is significantly longer than in **PH** (1.6 Å) (Figure 2) and in **PH·CH$_3$CN** (2.1 Å). Molecular water provides a bridge between the protic and hydridic hydrogens, thus facilitating the H−H bond formation. In the case of [CpRu(PTA)$_2$Cl],[31] the proton acceptor (PTA, a tertiary amine function) and the hydridic hydrogen are even further separated, and at least three water molecules are necessary to bridge them and make the process possible. In contrast, in **PH** the very short H^+/H^- distance makes it possible to have an efficient direct hydrogen formation without the need of an additional species to facilitate the proton movement.

Molecular water does not accelerate the H−H bond formation in H_2 production catalysts. Yet the overall catalytic rates for this class of catalysts have been observed to be significantly higher when water is present. Our results imply that H−H bond formation is not rate-determining and that molecular water accelerates other elementary steps along the catalytic cycle to improve the overall catalysis. In recent studies,[47,77,79−81] it has been shown that three different isomers are produced in reactions of the $[Ni(P^R_2N^{R'}_2H)_2]^{2+}$ catalysts. Only one isomer features protonated pendant amines with protons properly positioned for catalysis.[6] In addition, it has been found that proton delivery to the catalysts (for H_2 production) and proton removal from the catalysts (in H_2 oxidation) appear to be bottlenecks to catalysis in dry conditions.[48] These observations suggest that water may facilitate proton delivery (or removal) by directing protons to the right position and/or reducing protonation/deprotonation barriers. This hypothesis is consistent also with the recent observation that the rate enhancement due to water is more pronounced for bulky R′ groups and/or when bulkier acids are used.[7] A series of theoretical studies aimed at clarifying the role of water is currently in progress.[36,37]

Last, we note that the present results offer a new perspective on the role of molecular water for H_2 oxidation by similar $[Ni(P^R_2N^{R'}_2)_2]^{2+}$ catalysts. Table 1 and Figure 6 illustrate the point that for the reverse reaction **A** to **PH**, which is a step in the oxidation of H_2, the splitting of the H−H bond is facilitated by molecular waters acting as shuttles as they lower the reverse activation barrier.

■ ASSOCIATED CONTENT

Supporting Information

A discussion on the thermodynamic cycle used for the calculation of solvation free energies, structures of the dihydrogen adduct in the presence of water or acetonitrile in the catalytic pocket, and Cartesian coordinates of all stationary points. This information is available free of charge via the Internet at http://pubs.acs.org.

■ AUTHOR INFORMATION

Corresponding Author

*E-mail: simone.raugei@pnnl.gov, michel.dupuis@pnnl.gov.

Notes

The authors declare no competing financial interest.

■ ACKNOWLEDGMENTS

This research was supported as part of the Center for Molecular Electrocatalysis, an Energy Frontier Research Center funded by the US Department of Energy, Office of Science, Office of Basic Energy Sciences. Computational resources were provided at W. R. Wiley Environmental Molecular Science Laboratory—Pacific Northwest National Laboratory, the National Energy Research Scientific Computing Center (NERSC) at Lawrence Berkeley National Laboratory, and the Jaguar supercomputer at Oak Ridge National Laboratory.

■ REFERENCES

(1) Rakowski DuBois, M.; DuBois, D. L. *Acc. Chem. Res.* **2009**, *42*, 1974−1982.

(2) DuBois, D. L.; Bullock, R. M. *Eur. J. Inorg. Chem.* **2011**, *2011*, 1017−1027.

(3) Rakowski DuBois, M.; DuBois, D. L. *Chem. Soc. Rev.* **2009**, *38*, 62−72.

(4) We use the expression "molecular water(s)" to refer to specific water molecules that have particular properties or play particular roles in systems of interest (specific interactions with a solute or active

participation in a reaction mechanism). In nonaqueous solvents, molecular waters would come from a concentration of water molecules in a mixture. In an aqueous solvent, a molecular water might refer to a water from the first shell, for example, in contrast to water molecules in the bulk, or to water molecules that may be involved in specific elementary reactions.

(5) Stewart, M. P.; Ho, M.; Wiese, S.; Lindstrom, M. L.; Thogerson, C. E.; Raugei, S.; Bullock, R. M.; Helm, M. L. *J. Am. Chem. Soc.* **2013**, *135*, 6033−6046.
(6) Appel, A.; Pool, D.; O'Hagan, M.; Shaw, W.; Yang, J.; Rakowski DuBois, M.; DuBois, D.; Bullock, R. M. *ACS Catal.* **2011**, *1*, 777−785.
(7) Kilgore, U. J.; Roberts, J. A.; Pool, D. H.; Appel, A. M.; Stewart, M. P.; Rakowski DuBois, M.; Dougherty, W. G.; Kassel, W. S.; Bullock, R. M.; DuBois, D. L. *J. Am. Chem. Soc.* **2011**, *133*, 5861−5872.
(8) Helm, M. L.; Stewart, M. P.; Bullock, R. M.; Rakowski DuBois, M.; DuBois, D. L. *Science* **2011**, *333*, 863−866.
(9) Kubas, G. J. *Science* **2006**, *314*, 1096−1097.
(10) Kubas, G. J. *Acc. Chem. Res.* **1988**, *21*, 120−128.
(11) Kubas, G. J. *Chem. Rev.* **2007**, *107*, 4152−4205.
(12) Wilson, A. D.; Newell, R. H.; McNevin, M. J.; Muckerman, J. T.; Rakowski DuBois, M.; DuBois, D. L. *J. Am. Chem. Soc.* **2006**, *128*, 358−366.
(13) Small, Y. A.; DuBois, D. L.; Fujita, E.; Muckerman, J. T. *Energy Environ. Sci.* **2011**, *4*, 3008−3020.
(14) Wang, M.; Chen, L.; Sun, L. *Energy Environ. Sci.* **2012**, *5*, 6763−6778.
(15) Gloaguen, F.; Rauchfuss, T. B. *Chem. Soc. Rev.* **2009**, *38*, 100−108.
(16) Du, P.; Eisenberg, R. *Energy Environ. Sci.* **2012**, *5*, 6012−6021.
(17) Stephan, D.; Erker, G. *Angew. Chem., Int. Ed.* **2010**, *49*, 46−76.
(18) Stephan, D. W. *Org. Biomol. Chem.* **2008**, *6*, 1535−1539.
(19) Welch, G. C.; San Juan, R. R.; Masuda, J. D.; Stephan, D. W. *Science* **2006**, *314*, 1124−1126.
(20) Szymczak, N. K.; Tyler, D. R. *Coord. Chem. Rev.* **2008**, *252*, 212−230.
(21) Kovacs, G.; Rossin, A.; Gonsalvi, L.; Lledos, A.; Peruzzini, M. *Organometallics* **2010**, *29*, 5121−5131.
(22) Singleton, M. L.; Crouthers, D. J.; Duttweiler, R. P., III; Reibenspies, J. H.; Darensbourg, M. Y. *Inorg. Chem.* **2011**, *50*, 5015−5026.
(23) Karunadasa, H. I.; Chang, C. J.; Long, J. R. *Nature* **2010**, *464*, 1329−1333.
(24) Karunadasa, H.; Montalvo, E.; Sun, Y.; Majda, M.; Long, J.; Chang, C. *Science* **2012**, *335*, 698−702.
(25) Bianco, R.; Hynes, J. T. *Acc. Chem. Res.* **2006**, *39*, 159−165.
(26) Lim, C.; Holder, A.; Musgrave, C. *J. Am. Chem. Soc.* **2012**, *135*, 142−154.
(27) Belkova, N. V.; Epstein, L. M.; Shubina, E. S. *Eur. J. Inorg. Chem.* **2010**, *2010*, 3555−3565.
(28) Chandrasekhar, J.; Jorgensen, W. *J. Am. Chem. Soc.* **1985**, *107*, 2974−2975.
(29) Chandrasekhar, J.; Smith, S.; Jorgensen, W. *J. Am. Chem. Soc.* **1984**, *106*, 3049−3050.
(30) Chandrasekhar, J.; Smith, S.; Jorgensen, W. *J. Am. Chem. Soc.* **1985**, *107*, 154−163.
(31) Rossin, A.; Gonsalvi, L.; Phillips, A. D.; Maresca, O.; Lledós, A.; Peruzzini, M. *Organometallics* **2007**, *26*, 3289−3296.
(32) Li, J.; Shiota, Y.; Yoshizawa, K. *J. Am. Chem. Soc.* **2009**, *131*, 13584−13585.
(33) Sandhya, K. S.; Suresh, C. H. *Organometallics* **2011**, *30*, 3888−3891.
(34) Kohl, S. W.; Weiner, L.; Schwartsburd, L.; Konstantinovski, L.; Shimon, L. J.; Ben-David, Y.; Iron, M. A.; Milstein, D. *Science* **2009**, *324*, 74−77.
(35) Yang, J. Y; Smith, S. E.; Liu, T.; Dougherty, W. G.; Hoffert, W. A.; Kassel, W. S.; Rakowski DuBois, M.; DuBois, D. L.; Bullock, R. M. *J. Am. Chem. Soc.* **2013**, *135*, 9700−9712.
(36) Kilgore, U. J.; Stewart, M. P.; Helm, M. L.; Dougherty, W. G.; Kassel, W. S.; Rakowski, Dubois, M.; DuBois, D. L.; Bullock, R. M. *Inorg. Chem.* **2011**, *50*, 10908−10918.
(37) Wiese, S.; Kilgore, U. J.; DuBois, D. L.; Bullock, R. M. *ACS Catal.* **2012**, *2*, 720−727.
(38) Fontecilla-Camps, J. C.; Volbeda, A.; Cavazza, C.; Nicolet, Y. *Chem. Rev.* **2007**, *107*, 4273−4303.
(39) Shima, S.; Pilak, O.; Vogt, S.; Schick, M.; Stagni, M. S.; Meyer-Klaucke, W.; Warkentin, E.; Thauer, R. K.; Ermler, U. *Science* **2008**, *321*, 572−575.
(40) Volbeda, A.; Garcin, E.; Piras, C.; De Lacey, A. L.; Fernandez, V. M.; Hatchikian, E. C.; Frey, M.; Fontecilla-Camps, J. C. *J. Am. Chem. Soc.* **1996**, *118*, 12989−12996.
(41) Hoffert, W. A.; Roberts, J. A. S.; Bullock, R. M.; Helm, M. L. *Chem. Commun.* [Online] DOI: 10.1039/C3CC43203C.
(42) Yang, J. Y.; Chen, S.; Dougherty, W. G.; Kassel, W. S.; Bullock, R. M.; DuBois, D. L.; Raugei, S.; Rousseau, R.; Dupuis, M.; Rakowski DuBois, M. *Chem. Commun.* **2010**, *46*, 8618−8620.
(43) Chen, S.; Raugei, S.; Rousseau, R.; Dupuis, M.; Bullock, R. M. *J. Phys. Chem. A* **2010**, *114*, 12716−12724.
(44) Huynh, M. H.; Meyer, T. J. *Chem. Rev.* **2007**, *107*, 5004−5064.
(45) Mayer, J. M. *Annu. Rev. Phys. Chem.* **2004**, *55*, 363−390.
(46) Hammes-Schiffer, S.; Stuchebrukhov, A. A. *Chem. Rev.* **2010**, *110*, 6939−6960.
(47) O'Hagan, M.; Shaw, W. J.; Raugei, S.; Chen, S.; Yang, J. Y.; Kilgore, U. J.; DuBois, D. L.; Bullock, R. M. *J. Am. Chem. Soc.* **2011**, *133*, 14301−14312.
(48) O'Hagan, M.; Ho, M.-H.; Yang, J. Y.; Appel, A. M.; Rakowski DuBois, M.; Raugei, S.; Shaw, W. J.; DuBois, D. L.; Bullock, R. M. *J. Am. Chem. Soc.* **2012**, *134*, 19409−19424.
(49) Raugei, S.; Chen, S.; Ho, M.-H.; Ginovska-Pangovska, B.; Rousseau, R. J.; Dupuis, M.; DuBois, D. L.; Bullock, R. M. *Chem.—Eur. J.* **2012**, *18*, 6493−6506.
(50) Warshel, A.; Levitt, M. *J. Mol. Biol.* **1976**, *103*, 227−249.
(51) Perdew, J. P. *Phys. Rev. B* **1986**, *33*, 8822−8824.
(52) Becke, A. D. *J. Chem. Phys.* **1993**, *98*, 5648−5652.
(53) Andrae, D.; Haubermann, U.; Dolg, M.; Stoll, H.; Preub, H. *Theor. Chim. Acta* **1990**, *77*, 123−141.
(54) Rassolov, V. A.; Pople, J. A.; Ratner, M. A.; Windus, T. L. *J. Chem. Phys.* **1998**, *109*, 1223−1229.
(55) Cossi, M.; Rega, N.; Scalmani, G.; Barone, V. *J. Comput. Chem.* **2003**, *24*, 669−681.
(56) Barone, V.; Cossi, M. *J. Phys. Chem. A* **1998**, *102*, 1995−2001.
(57) Bondi, A. *J. Phys. Chem.* **1964**, *68*, 441−451.
(58) Fukui, K. *Acc. Chem. Res.* **1981**, *14*, 363−368.
(59) Frisch, M. J.; Trucks, G. W.; Schlegel, H. B.; Scuseria, G. E.; Robb, M. A.; Cheeseman, J. R.; Scalmani, G.; Barone, V.; Mennucci, B.; Petersson, G. A.; Nakatsuji, H.; Caricato, M.; Li, X.; Hratchian, H. P.; Izmaylov, A. F.; Bloino, J.; Zheng, G.; Sonnenberg, J. L.; Hada, M.; Ehara, M.; Toyota, K.; Fukuda, R.; Hasegawa, J.; Ishida, M.; Nakajima, T.; Honda, Y.; Kitao, O.; Nakai, H.; Vreven, T.; Montgomery, J. A., Jr.; Peralta, J. E.; Ogliaro, F.; Bearpark, M.; Heyd, J. J.; Brothers, E.; Kudin, K. N.; Staroverov, V. N.; Kobayashi, R.; Normand, J.; Raghavachari, K.; Rendell, A.; Burant, J. C.; Iyengar, S. S.; Tomasi, J.; Cossi, M.; Rega, N.; Millam, J. M.; Klene, M.; Knox, J. E.; Cross, J. B.; Bakken, V.; Adamo, C.; Jaramillo, J.; Gomperts, R.; Stratmann, R. E.; Yazyev, O.; Austin, A. J.; Cammi, R.; Pomelli, C.; Ochterski, J. W.; Martin, R. L.; Morokuma, K.; Zakrzewski, V. G.; Voth, G. A.; Salvador, P.; Dannenberg, J. J.; Dapprich, S.; Daniels, A. D.; Farkas, Ö.; Foresman, J. B.; Ortiz, J. V.; Cioslowski, J.; Fox, D. J. Gaussian, Inc.: Wallingford, CT, 2009.
(60) Klamt, A.; Mennucci, B.; Tomasi, J.; Barone, V.; Curutchet, C.; Orozco, M.; Luque, F. J. *Acc. Chem. Res.* **2009**, *42*, 489−492.
(61) Cramer, C. J.; Truhlar, D. G. *Acc. Chem. Res.* **2008**, *41*, 760−768.
(62) Pliego, J. R.; Riveros, J. M. *J. Phys. Chem. A* **2001**, *105*, 7241−7247.
(63) Bryantsev, V. S.; Diallo, M. S.; Goddard, W. A., III. *J. Phys. Chem. B* **2008**, *112*, 9709−9719.
(64) Parrinello, M.; Rahman, A. *J. App. Phys.* **1981**, *52*, 7182−7190.

(65) Martyna, G. J.; Klein, M. L.; Tuckerman, M. *J. Chem. Phys.* **1992**, *97*, 2635−2643.
(66) Wang, J.; Wolf, R. M.; Caldwell, J. W.; Kollman, P. A.; Case, D. A. *J. Comput. Chem.* **2004**, *25*, 1157−1174.
(67) Laino, T.; Mohamed, F.; Laio, A.; Parrinello, M. *J. Chem. Theory Comput.* **2006**, *2*, 1370−1378.
(68) VandeVondele, J.; Krack, M.; Mohamed, F.; Parrinello, M.; Chassaing, T.; Hutter, J. *Comput. Phys. Commun.* **2005**, *167*, 103−128.
(69) VandeVondele, J.; Hutter, J. *J. Chem. Phys.* **2007**, *127*, 114105−10.
(70) Goedecker, S.; Teter, M.; Hutter, J. *Phys. Rev. B* **1996**, *54*, 1703−1710.
(71) Perdew, J. P.; Burke, K.; Ernzerhof, M. *Phys. Rev. Lett.* **1996**, *77*, 3865−3868.
(72) Grimme, S. *J. Comput. Chem.* **2004**, *25*, 1463−1473.
(73) Nikitin, A. M.; Lyubartsev, A. P. *J. Comput. Chem.* **2007**, *28*, 2020−2026.
(74) Jorgensen, W. L.; Chandrasekhar, J.; Madura, J. D.; Impey, R. W.; Klein, M. L. *J. Chem. Phys.* **1983**, *79*, 926.
(75) Sprik, M.; Ciccotti, G. *J. Chem. Phys.* **1998**, *109*, 7737−7744.
(76) Dill, K. A.; Bromberg, S. *Molecular Driving Forces*; Garland Pub: New York, 2002.
(77) Fraze, K.; Wilson, A. D.; Appel, A. M.; Rakowski DuBois, M.; DuBois, D. L. *Organometallics* **2007**, *26*, 3918−3924.
(78) Agmon, N. *Chem. Phys. Lett.* **1995**, *244*, 456−462.
(79) Wilson, A. D.; Shoemaker, R. K.; Miedaner, A.; Muckerman, J. T.; DuBois, D. L.; Rakowski DuBois, M. *Proc. Natl. Acad. Sci. U. S. A.* **2007**, *104*, 6951−6956.
(80) Smith, S. E.; Yang, J. Y.; DuBois, D. L.; Bullock, R. M. *Angew. Chem., Int. Ed.* **2012**, *51*, 3152−3155.
(81) Wiedner, E. S.; Yang, J. Y.; Chen, S.; Raugei, S.; Dougherty, W. G.; Kassel, W. S.; Helm, M. L.; Bullock, R. M.; Rakowski DuBois, M.; Daniel, D. L. *Organometallics* **2011**, *31*, 144−156.